Received: 23 January 2022 | Revised: 1 November 2022 | Accepted: 3 November 2022

DOI: 10.1002/pld3.467

ORIGINAL RESEARCH

Metabolic network changes during skotomorphogenesis in *Arabidopsis thaliana* mutant (*atdfb-3*)

Xingjuan Li[1] | Hongyan Meng[2] | Liqing Liu[2] | Cuiyun Hong[2] | Chunyi Zhang[3]

[1]College of Bioengineering, Beijing Polytechnic, Beijing, China

[2]Fujian Provincial Key Laboratory of Subtropical Plant Physiology and Biochemistry, Fujian Institute of Subtropical Botany, Xiamen, China

[3]Biotechnology Research Institute, Chinese Academy of Agricultural Sciences, Beijing, China

Correspondence
Xingjuan Li, College of Bioengineering, Beijing Polytechnic, Liangshuihe 1st Street NO.9, Yizhuang Economic and Technological Development Zone, Beijing, China, 100176.
Email: lixingjuan@bpi.edu.cn

Funding information
This work was supported by the Research on National Reference Material and Product Development of Natural Products (No. SG030801), Major Science and Technology Project of Xiamen, China (No.3502Z20211004), National Natural Science Foundation of China (No. 31800245), and the Key Science and Technology Programs of Beijing Polytechnic (No. 2020Z113-KXZ).

Abstract

The metabolic networks underlying skotomorphogenesis in seedlings remain relatively unknown. On the basis of our previous study on the folate metabolism in seedlings grown in darkness, the plastidial folylpolyglutamate synthetase gene (*AtDFB*) T-DNA insertion *Arabidopsis thaliana* mutant (*atdfb-3*) was examined. Under the nitrate-sufficient condition, the mutant exhibited deficient folate metabolism and hypocotyl elongation, which affected skotomorphogenesis. Further analyses revealed changes to multiple intermediate metabolites related to carbon and nitrogen metabolism in the etiolated *atdfb-3* seedlings. Specifically, the sugar, polyol, and fatty acid contents decreased in the *atdfb-3* mutant under the nitrate-sufficient condition, whereas the abundance of various organic acids and amino acids increased. In response to nitrate-limited stress, multiple metabolites, including sugars, polyols, fatty acids, organic acids, and amino acids, accumulated more in the mutant than in the wild-type control. The differences in the contents of multiple metabolites between the *atdfb-3* and wild-type seedlings decreased following the addition of exogenous 5-F-THF under both nitrogen conditions. Additionally, the mutant accumulated high levels of one-carbon metabolites, such as Cys, S-adenosylmethionine, and S-adenosylhomocysteine, under both nitrogen conditions. Thus, our data demonstrated that the perturbed folate metabolism in the *atdfb-3* seedlings, which was caused by the loss-of-function mutation to *AtDFB*, probably altered carbon and nitrogen metabolism, thereby modulating skotomorphogenesis. Furthermore, the study findings provide new evidence of the links among folate metabolism, metabolic networks, and skotomorphogenesis.

KEYWORDS
Arabidopsis, folate, metabolic networks, skotomorphogenesis

Xingjuan Li and Hongyan Meng contributed equally to this work.

1 | INTRODUCTION

Seedlings grown in darkness exhibit skotomorphogenesis, which is characterized by the formation of apical hooks, closed cotyledon, and hypocotyl elongation (Jin et al., 2021; Josse & Halliday, 2008). Metabolism plays an important role in seedling development during skotomorphogenesis. In *Arabidopsis thaliana*, carbon metabolism is important for skotomorphogenesis. Triacylglycerol, which is the main form of lipid stored in seeds, is catabolized to yield free fatty acids and glycerol, both of which are ultimately converted to sugars that are required for post-germination seedling growth in darkness (Chen & Thelen, 2010; Liu et al., 2017; O'Neill et al., 2003). A deficiency in galactose synthesis in the Arabidopsis *mur3-3* mutant results in the production of dysfunctional xyloglucan. The mutant plants exhibit decreased hypocotyl cell elongation (Xu et al., 2017). Sucrose stimulates seedling hypocotyl elongation in darkness in a gibberellin-dependent manner and restores the wild-type hypocotyl phenotype in the short-hypocotyl mutants *icl* and *pck1* (Eastmond et al., 2000; Li et al., 2019; Penfield et al., 2004; Zhang et al., 2010). Additionally, the effects of glucose and cytokinin signaling are reportedly integrated to control hypocotyl length in skotomorphogenesis (Kushwah & Laxmi, 2014). The accumulation of carbohydrates, especially starch, is related to nitrogen metabolism during plant growth and development (Zhong et al., 2021). Moreover, nitrogen metabolism is essential for hypocotyl growth. In dark-grown conifer plants, some of the nitrogen mobilized from the megagametophyte is directed toward the hypocotyl soon after germination for the production of a large amount of Asn that serves as a reservoir of nitrogen to satisfy the subsequent specific demands of developmental activities (Canas et al., 2006). Furthermore, γ-aminobutyric acid (γ-Aba) inhibits hypocotyl elongation during Arabidopsis skotomorphogenesis (Renault et al., 2011).

Folates comprise tetrahydrofolate and its derivatives. Folylpolyglutamate derivatives are central cofactors for folate-dependent enzymes (Hanson & Gregory, 2002; Hanson & Gregory, 2011; Hanson & Roje, 2001; Ravanel et al., 2001; Sahr et al., 2005; Van Wilder et al., 2009). There is a substantial accumulation of folate after seed germination, reaching peak levels on the fifth day (Sallam et al., 2021). Mutations in genes involved in folate synthesis result in altered photorespiration and the depletion of amino acids, nucleotides, and seed fatty acid methyl esters (Collakova et al., 2008; Goyer et al., 2005; Jiang et al., 2013; Srivastava et al., 2011). Folates are important for nitrogen utilization and plant resistance to low-nitrogen stress (Jiang et al., 2013). A mutation to *AtDFC*, which encodes a mitochondrial folylpolyglutamate synthetase (FPGS), leads to altered nitrogen metabolism and pronounced phenotypes in response to low-nitrogen stress (Jiang et al., 2013). A mutation to *AtDFB*, which encodes a plastidial FPGS isoform, modulates the glutamylation status of some folates and broadly alters metabolism under both dark and light conditions (Hayashi et al., 2017; Meng et al., 2014; Meng et al., 2017; Srivastava et al., 2011). Folate polyglutamylation is also required for global DNA methylation and histone H3 lysine 9 dimethylation through its function related to one-carbon metabolism (Zhou et al., 2013). Sulfamethazine, a chemical suppressor of epigenetic silencing, decreases the plant folate content and causes methyl deficiency, as demonstrated by decreased S-adenosylmethionine (SAM) levels and global DNA methylation (Zhang et al., 2012). These earlier studies indicated that complex folate-regulated metabolic networks are present in plants; however, the interactions between folate metabolism and other metabolic pathways, and how the interactions are affected by limited nitrogen availability during skotomorphogenesis, remain relatively unknown.

In our previous study (Meng et al., 2014; Meng et al., 2017), defects in hypocotyl elongation, folate metabolism, and nitrogen metabolism were observed in etiolated *atdfb-3* seedlings, in which T-DNA was inserted into the plastidial FPGS gene (*AtDFB*), under nitrate-sufficient conditions; the defects were enhanced under nitrate-limited conditions. The complementary lines were phenotypically the same as the wild-type control under both nitrogen levels. The application of 5-F-THF effectively restored the hypocotyl length of the dark-grown *atdfb-3* seedlings to the wild-type level and completely restored the nitrogen, soluble protein, nitrate, and endogenous 5-F-THF contents in *atdfb-3* seedlings to the wild-type levels under nitrate-limited conditions in darkness.

In this study, etiolated *atdfb-3* seedlings were defective in terms of multiple metabolites, including sugars, polyols, fatty acids, organic acids, amino acids, and one-carbon metabolites. Our data indicate that changes to metabolic networks were probably induced by the perturbed folate metabolism due to a loss-of-function mutation to *AtDFB*. The data presented herein provide new evidence of the relationships among folate metabolism, metabolic networks, and skotomorphogenesis.

2 | MATERIALS AND METHODS

2.1 | Plant materials and growth conditions

In this study, nitrate was used as the sole nitrogen source. The nitrate-sufficient and nitrate-limited conditions were set as 9.4-mM NO_3^- (9.4 N) and .3-mM NO_3^- (.3 N), respectively. The 5-mM 5-F-THF stock solution was added to 9.4- and .3-N media for a working concentration of 50-μM 5-F-THF. The resulting media were designated as 9.4 N + 5-F-THF and .3 N + 5-F-THF. Seeds of the Arabidopsis wild-type control (*A. thaliana*, ecotype Columbia), the T-DNA mutant (i.e., *atdfb-3*) with an insertion in the sixth intron of the At5g05980 gene (SALK_015472), which encodes the plastidial FPGS isoform designated as AtDFB, and the *AtDFB* complementary (COM) line (Pro*AtDFB*:*AtDFB* complementary vector inserted into the *atdfb-3* mutant) were sterilized, added to plates containing the above-mentioned media, and incubated at 4°C in darkness for 2 days. The plates were then moved to a growth chamber and incubated at 22°C in darkness for 6 days (Meng et al., 2014). The hypocotyls of the 6-day-old etiolated seedlings were

photographed using the Nikon 700 camera. Hypocotyl lengths were measured using ImageJ.

2.2 | Seedling metabolite profile analysis

Six-day-old etiolated wild-type, *atdfb-3*, and COM seedlings from the 9.4 N, .3 N, 9.4 N + 5-F-THF, and .3 N + 5-F-THF medium plates were collected and immediately frozen in liquid nitrogen for the subsequent profiling of metabolites, including sugars, polyols, fatty acids, and organic acids, using a gas chromatography time-of-flight mass spectrometry (GC-TOF-MS) system. Samples were prepared, metabolites were measured, and data were analyzed as previously described (Meng et al., 2014).

2.3 | Real-time RT-PCR expression analysis

Six-day-old etiolated wild-type, and *atdfb-3* seedlings from the three 9.4 N, and .3-N medium plates were respectively collected and immediately frozen in liquid nitrogen for total RNA extraction. Total RNA was isolated from whole seedlings using HiPure Plant RNA Mini Kit (Magen). Reverse transcription was performed using PrimeScript RT reagent Kit (TaKaRa). The transcripts were amplified using Hieff® qPCR SYBR Green Master Mix (Yeasen) with Roche Applied Science Light Cycler 96. Real-time quantitative PCR experiments were repeated independently for three times. For relative quantification values for each target gene were calculated by the $2^{-\Delta\Delta CT}$ method. *ACTIN2* was used as an internal control, and control treatment (WT seedlings on 9.4-N medium) was normalized to a value of 1.00. The primers used in this study are listed in Table S1.

2.4 | Amino acid and one-carbon metabolite analyses

Six-day-old etiolated wild-type, *atdfb-3*, and COM seedlings from the 9.4 N, .3 N, 9.4 N + 5-F-THF, and .3 N + 5-F-THF medium plates were used for analyzing the free amino acids and one-carbon metabolites, including Hcy, Cys, SAM, and S-adenosylhomocysteine (SAH). Samples were prepared and metabolite contents were measured as previously described (Meng et al., 2014; Nikiforova et al., 2005; Zhou et al., 2013).

2.5 | Accession numbers

The sequence data in this article can be found in the Arabidopsis Genome Initiative or GenBank/EMBL databases under the following accession numbers: AT5G05980 (*AtDFB*), AT3G18780 (*ACTIN2*), AT2G34590 (*PDH-E1β*), AT1G74690 (*KASII*), AT3G25110 (*FatA*), AT4G34520 (*FAE1*), AT4G29010 (*AIM1*), AT3G15290 (*HCDH*), AT2G33150 (*KAT2*), and AT5G48880 (*KAT5*).

3 | RESULTS

3.1 | Carbon metabolites are affected by the *AtDFB* mutation

We investigated the post-germination growth of the wild-type, *atdfb-3*, and COM seedlings incubated in darkness for 6 days under nitrate-sufficient and nitrate-limited conditions. In an earlier study, the wild-type and mutant seedlings on the 9.4-N medium were phenotypically similar to the corresponding seedlings on half-strength MS medium (30-N nitrogen supply containing 10.3-mM [NH_4NO_3] and 9.4-mM KNO_3) (Meng et al., 2014). Thus, the 9.4-N (9.4-mM NO_3^-) medium was used as the nitrate-sufficient condition in this study. On the 9.4-N medium, the *atdfb-3* seedlings had shorter hypocotyls and primary roots as well as more expanded cotyledon and a greater apical hook curvature than the wild-type control. The hypocotyl and primary root phenotypes of the COM seedlings were similar to the wild-type control (Figure S1). Under the nitrate-limited condition, the hypocotyl and primary root phenotypes differed significantly between the *atdfb-3* and wild-type seedlings. The mutant had a substantially shortened hypocotyl that was only 30% of the wild-type hypocotyl length. In contrast, the hypocotyl and primary root phenotypes of the wild-type and COM seedlings were similar to those of the seedlings grown on the 9.4-N medium. The *atdfb-3* and COM cotyledons were folded similarly to those of the wild-type; however, the apical hook curvature was greater for *atdfb-3* than for the wild-type control. Because the elongation of the *atdfb-3* hypocotyl was significantly inhibited by .3 N (.3-mM NO_3^-), .3 N was used as the nitrate-limited condition. The above-mentioned results indicated that compared with the wild-type and COM seedlings, the *atdfb-3* seedlings had a shorter hypocotyl; this difference was greater under the nitrate-limited condition than under the nitrate-sufficient condition in darkness. The addition of exogenous 5-F-THF effectively restored the hypocotyl length of the dark-grown *atdfb-3* seedlings to the wild-type level (Meng et al., 2014; Meng et al., 2017). To explore whether altered folate metabolism affects metabolic networks, we used a GC-TOF-MS system to analyze the etiolated seedling metabolite profiles of the three genotypes (wild-type, *atdfb-3*, and COM) in response to different external nitrate levels and without or with 5-F-THF.

The analyzed carbon metabolites (i.e., nine sugars, five polyols, nine organic acids, 18 fatty acids, and 22 other organic compounds) are listed in Tables S2–S6 and S9–S13.

3.1.1 | Analysis of the sugars affected by the *AtDFB* mutation

When the external nitrogen level was sufficient, the loss-of-function mutation to *AtDFB* significantly decreased the abundance of various sugars (Figure 1a and Table S2). Specifically, the galactopyranoside, glucopyranoside, mannose, and xylopyranose contents in the *atdfb-3* seedlings were only 58%, 7%, 20%, and 65% of the corresponding wild-type levels, respectively. The content of some sugars in the COM

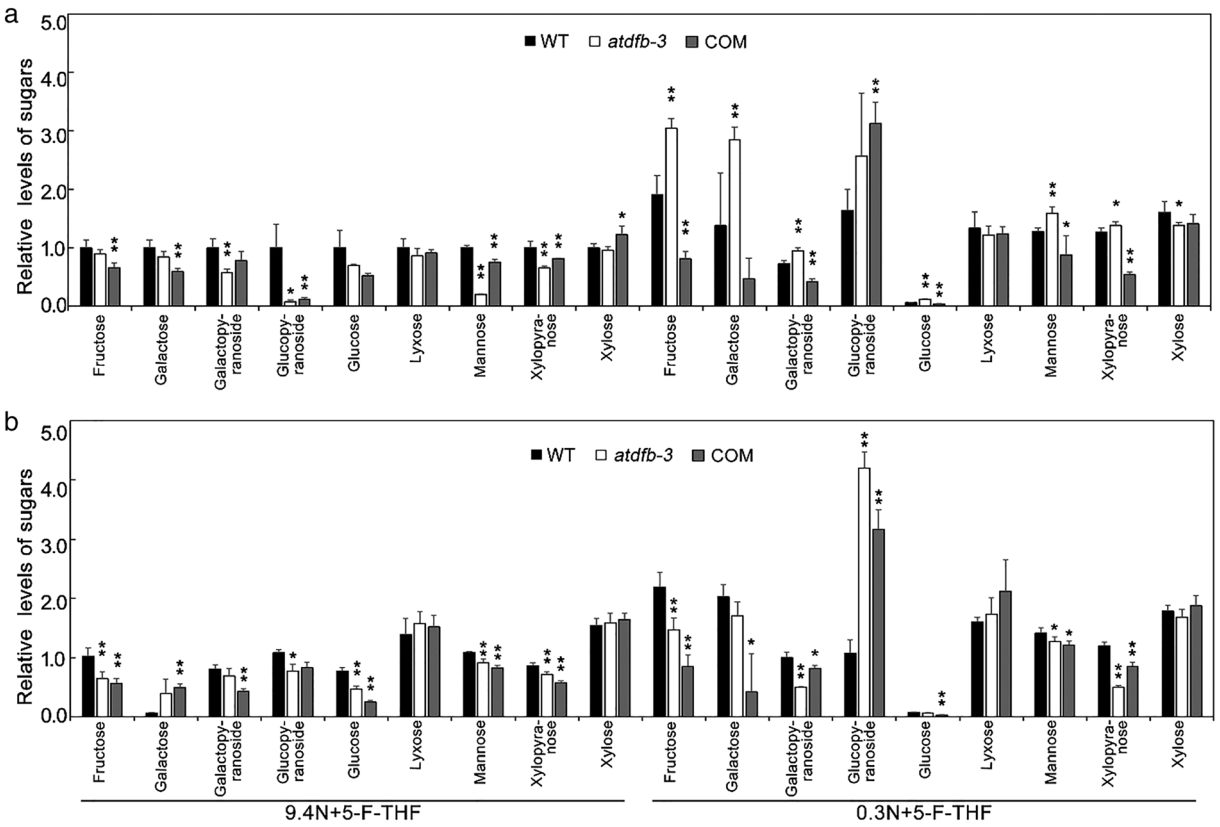

FIGURE 1 Relative levels of sugars in 6-day-old etiolated wild-type, *atdfb-3*, and *AtDFB* complemented (COM) seedlings on 9.4- or .3-N medium (a), and 9.4- or .3-N medium with 5-F-THF (b). $n = 5$, and each replicate consisted of 100-mg pooled plant material. White bars with * indicate significant differences at $P < .05$, and those with ** indicate highly significant differences at $P < .01$ (Student's *t*-test).

line, such as galactopyranoside, lyxose, mannose, and xylopyranose, had partially recovered to 75% of that in the wild-type control. We speculated that a lack of normal folate metabolism during skotomorphogenesis affected carbohydrate metabolism (Table S2). For all three genotypes, the fructose, glucopyranoside, lyxose, mannose, and xylose contents were higher under the nitrate-limited condition than under the nitrate-sufficient condition (Figure 1a and Table S2). Among the three genotypes, these sugars accumulated the most in *atdfb-3*. The glucopyranoside and mannose contents in the *atdfb-3* seedlings were respectively 35.71-fold and 6.95-fold higher under the .3-N condition than under the 9.4-N condition. Compared with the wild-type seedlings grown on the same condition, the fructose, galactose, galactopyranoside, mannose, and xylopyranose contents were higher in the *atdfb-3* seedlings under nitrate-limited condition, whereas the lyxose and xylose contents were lower. The galactose content in the *atdfb-3* mutant was 1.07-fold higher than in the wild-type control (Figure 1a and Table S2).

The glucopyranoside and mannose contents were respectively 10.00-fold and 3.60-fold higher in the *atdfb-3* seedlings on the 9.4 N + 5-F-THF medium than in the *atdfb-3* seedlings on the 9.4-N medium (Figure 1 and Table S2). The ratios of the glucopyranoside and mannose contents between the *atdfb-3* and wild-type seedlings were respectively .07 and .20 on the 9.4-N medium but were restored to .71 and .84 after the application of 5-F-THF. The lyxose and xylose contents were relatively similar among the three genotypes following the addition of 5-F-THF. Seedings grown on the .3-N condition with and without 5-F-THF supplementation, the differences of sugar content between the *atdfb-3* mutant and wild-type seedlings decreased (Figure 1 and Tables S2 & S9). For example, after the 5-F-THF supplementation, the galactose content decreased in the *atdfb-3* seedlings, but it increased in the wild-type seedlings. Accordingly, the ratio of the galactose content between the *atdfb-3* and wild-type seedlings was 2.07 under the .3-N condition, but was restored to .84 under the .3 N + 5-F-THF condition. The changes in the glucose, lyxose, mannose, and xylose contents between the *atdfb-3* and wild-type seedlings were similar. Regardless of the medium (i.e., 9.4 or .3 N), the addition of 5-F-THF decreased the differences in the sugar contents between the *atdfb-3* and wild-type seedlings (Figure 1 and Table S2). These results may reflect a direct link between folate metabolism and carbohydrate metabolism.

3.1.2 | Analysis of the polyols affected by the *AtDFB* mutation

The ribitol and stigmasterol contents in the *atdfb-3* mutant were only 75% and 47% of the wild-type levels, respectively, under the 9.4-N condition (Figure 2 and Table S3). For the seedlings grown on the

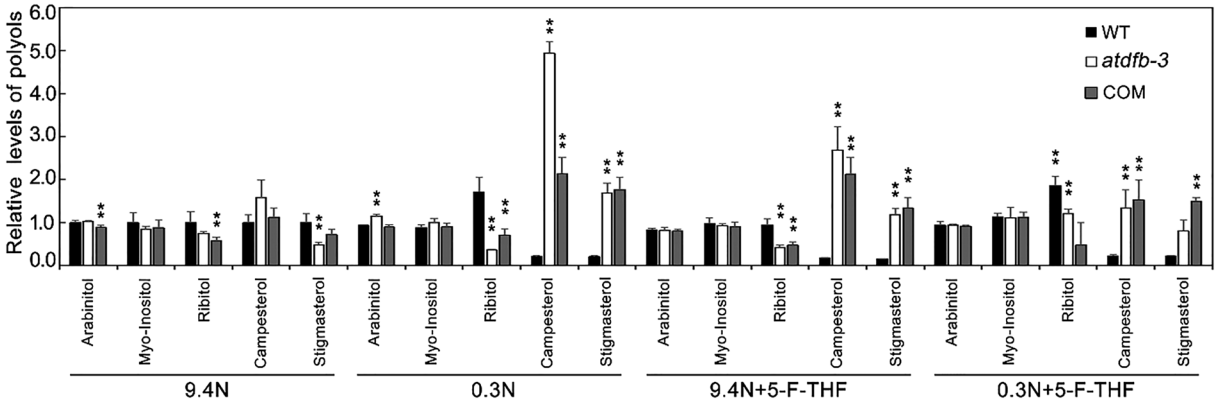

FIGURE 2 Relative levels of polyols in 6-day-old etiolated wild-type, *atdfb-3*, and *AtDFB* complemented (COM) seedlings on 9.4- or .3-N medium, and 9.4- or .3-N medium with 5-F-THF. $n = 5$, and each replicate consisted of 100-mg pooled plant material. White bars with * indicate significant differences at $P < .05$, and those with ** indicate highly significant differences at $P < .01$ (Student's *t*-test).

.3-N medium, the abundance of two polyols (campesterol and stigmasterol) decreased in the wild-type control, but substantially increased in the *atdfb-3* mutant. The campesterol and stigmasterol contents were respectively 22.52-fold and 7.45-fold higher in the *atdfb-3* seedlings than in the wild-type seedlings on the .3-N medium. In contrast, the ribitol content in the *atdfb-3* seedlings was only 21% of that in the wild-type seedlings under the .3-N condition (Figure 2 and Table S3). The addition of 5-F-THF to the 9.4-N medium altered the contents of two polyols (campesterol and stigmasterol), with a sharp decrease in the wild-type seedlings, but a considerable increase in the *atdfb-3* and COM seedlings (Figure 2). Consequently, the campesterol and stigmasterol contents were 13.89-fold and 6.87-fold higher in the mutant seedlings than in the wild-type seedlings. After adding 5-F-THF to the .3-N medium, there was no change in the campesterol and stigmasterol contents in the wild-type seedlings (compared with the seedlings grown on the .3-N medium), but there was a sharp decrease in the contents of the two polyols in the mutant seedlings. Hence, the ratios of the campesterol and stigmasterol contents between the mutant and wild-type seedlings were respectively 23.52 and 8.45 under the .3-N condition but were 6.09 and 3.64 after the addition of 5-F-THF. Supplementing the medium with 5-F-THF decreased the difference in the polyol contents between the *atdfb-3* and wild-type seedlings (Figure 2 and Tables S3 & S10).

3.1.3 | Analysis of the fatty acids affected by the *AtDFB* mutation

Among the 18 analyzed fatty acids, seven fatty acids (2:0, 3:0, 12:0, 13:0, 16:0, 20:0, and 24:0) in the *atdfb-3* mutant were significantly lower than those in the wild-type control under the 9.4-N condition, whereas there was no difference in the amount of two fatty acids (4:0, and 18:2) (Figure 3 and Table S4). The abundance of 15 fatty acids in the COM seedlings was restored to more than 75% of the corresponding amount in the wild-type seedlings. For the wild-type seedlings grown on the .3-N medium, the contents of 17 fatty acids decreased to varying degrees, whereas there was a slight increase in the 18:2 content. In response to the nitrate-limited stress treatment, the contents of two fatty acids (3:0 and 20:2) decreased in the *atdfb-3* mutant, but the abundance of 14 fatty acids increased significantly (Figure 3a and Table S4). Under the nitrate-limited condition, because of the loss-of-function mutation to *AtDFB*, fatty acids that were not converted into other substances or sugars to resist the effects of low-nitrogen stress like in the wild-type control accumulated in the *atdfb-3* seedlings. Therefore, we speculated that folate is involved in or regulates fatty acid conversion.

The addition of exogenous 5-F-THF to the 9.4-N medium resulted in the accumulation of 16 fatty acids in the *atdfb-3* seedlings to levels that were higher than the corresponding levels in the wild-type control (Figure 3b and Table S4). Compared with the mutant seedlings grown on the .3-N medium, the contents of most fatty acids decreased substantially in the *atdfb-3* mutant after 5-F-THF was added to the .3-N medium, but they changed only slightly in the wild-type, after 5-F-THF was added to the medium (Figure 3 and Tables S4 and S11). The ratios of the 18:3, 20:0, 20:1, 22:0, and 24:0 contents between the *atdfb-3* and wild-type seedlings were respectively 6.15, 4.89, 7.44, 4.21, and 10.90 under the .3-N condition but were restored to 1.20, 1.28, 3.77, 1.40, and 3.22 under the .3 N + 5-F-THF condition. Additionally, the ratio of the 20:2 content was .14 under the .3-N condition but was 1.25 under the .3 N + 5-F-THF condition. These findings suggest that the application of 5-F-THF decreased the differences in the contents of these fatty acids between the *atdfb-3* and wild-type seedlings (Figure 3 and Table S4). There may have been sufficient amounts of folate in the *atdfb-3* seedlings after the application of 5-F-THF. The sufficient amounts of folate in the *atdfb-3* mutant could convert other substances into fatty acids or convert fatty acids into other substances, including sugars, that serve as an energy source during skotomorphogenesis to restore hypocotyl elongation to normally the wild-type levels.

On the basis of the fatty acids with large changes in abundance, we selected genes involved in fatty acid biosynthesis, such as *PYRUVATE DEHYDROGENASE* (*PDH-E1β*; i.e., encoding the β-subunit of the

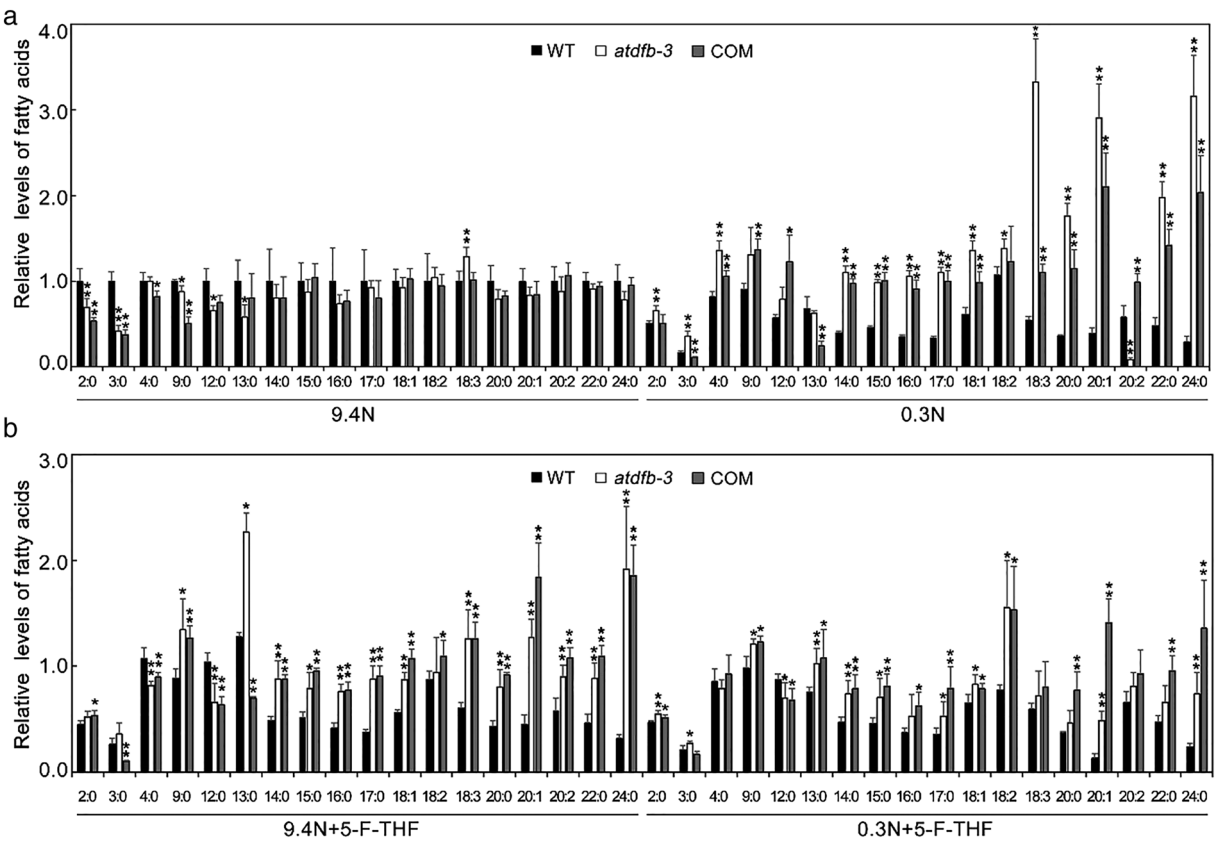

FIGURE 3 Relative levels of fatty acids in 6-day-old etiolated wild-type, *atdfb-3*, and *AtDFB* complemented (COM) seedlings on 9.4- or .3-N medium (a), and 9.4- or .3-N medium with 5-F-THF (b). Fatty acids included acetic acid (2:0), propanoic acid (3:0), butanoic acid (4:0), nonanoic acid (9:0), dodecanoic acid (12:0), tridecanoic acid (13:0), tetradecanoic acid (14:0), n-pentadecanoic acid (15:0), hexadecanoic acid (16:0), heptadecanoic acid (17:0), oleic acid (18:1), 9,12-octadecadienoic acid (18:2), linolenic acid (18:3), eicosanoic acid (20:0), 11-eicosenoic acid (20:1), 11,14-eicosadienoic acid (20:2), docosanoic acid (22:0), and tetracosanoic acid (24:0). $n = 5$, and each replicate consisted of 100-mg pooled plant material. White bars with * indicate significant differences at $P < .05$, and those with ** indicate highly significant differences at $P < .01$ (Student's *t*-test).

enzyme), *KETOACYL-ACP SYNTHASE II* (*KASII*), *ACYL-ACP THIOESTERASE* (*FatA*), and *FATTY ACID ELONGATION 1* (*FAE1*), as well as genes involved in β-oxidation, including *ABNORMAL INFLORESCENCE MERISTEM 1* (*AIM1*), *3-HYDROXYACYL-COA DEHYDROGENASE* (*HCDH*), *3-KETOACYL-COA THIOLASE 2* (*KAT2*), and *3-KETOACYL-COA THIOLASE 5* (*KAT5*), for an expression analysis. When the nitrogen availability was sufficient, the expression of *KAT5*, *FAE1*, and *FatA* was respectively 6.11-fold, 1.95-fold, and 1.15-fold higher in the mutant than in the wild-type seedlings. Under the low-nitrogen stress, the expression of *HCDH*, *FAE1*, and *FatA* was respectively 1.18-fold, 1.02-fold, and 1.18-fold higher in the mutant than in the wild-type seedlings (Figure S2). The low-nitrogen stress stimulated the expression of most genes in both genotypes, only that of *HCDH* in wild type under .3 N was lower compared to that in wild type under 9.4 N. For example, N limitation made the expression of *KAT5* in wild-type seedlings increased 15.13-fold higher than in the wild-type control grown on the 9.4-N condition, and it was 2.40-fold higher in *atdfb-3* seedings due to a loss-of-function mutation to *AtDFB* as compared with the mutant under 9.4-N condition (Figure S2). These results indicate that fatty acid biosynthesis and β-oxidation have been affected at the transcriptional level in the *atdfb-3* plants. In this study, the contents of multiple sugars, polyols, and fatty acids decreased in the *atdfb-3* mutant under the 9.4-N condition, but they increased substantially under the .3-N condition, probably because the loss-of-function mutation to *AtDFB* adversely influenced folate metabolism. When 5-F-THF was added to either medium (i.e., 9.4 or .3 N), the differences between the wild-type and mutant seedlings decreased significantly. More specifically, the contents of multiple sugars, polyols, and fatty acids in the *atdfb-3* seedlings were essentially restored to wild-type levels. These results reflect the importance of folate metabolism for carbon metabolism during skotomorphogenesis.

3.1.4 | Analysis of the organic acids affected by the *AtDFB* mutation

Unlike sugars, polyols, and fatty acids, the analyzed organic acids (e.g., butanedioic acid, ethanedioic acid, malic acid, pentanedioic acid, and propanedioic acid) accumulated in the *atdfb-3* seedlings under both nitrate conditions (Figure 4a and Table S5). The addition of 5-F-

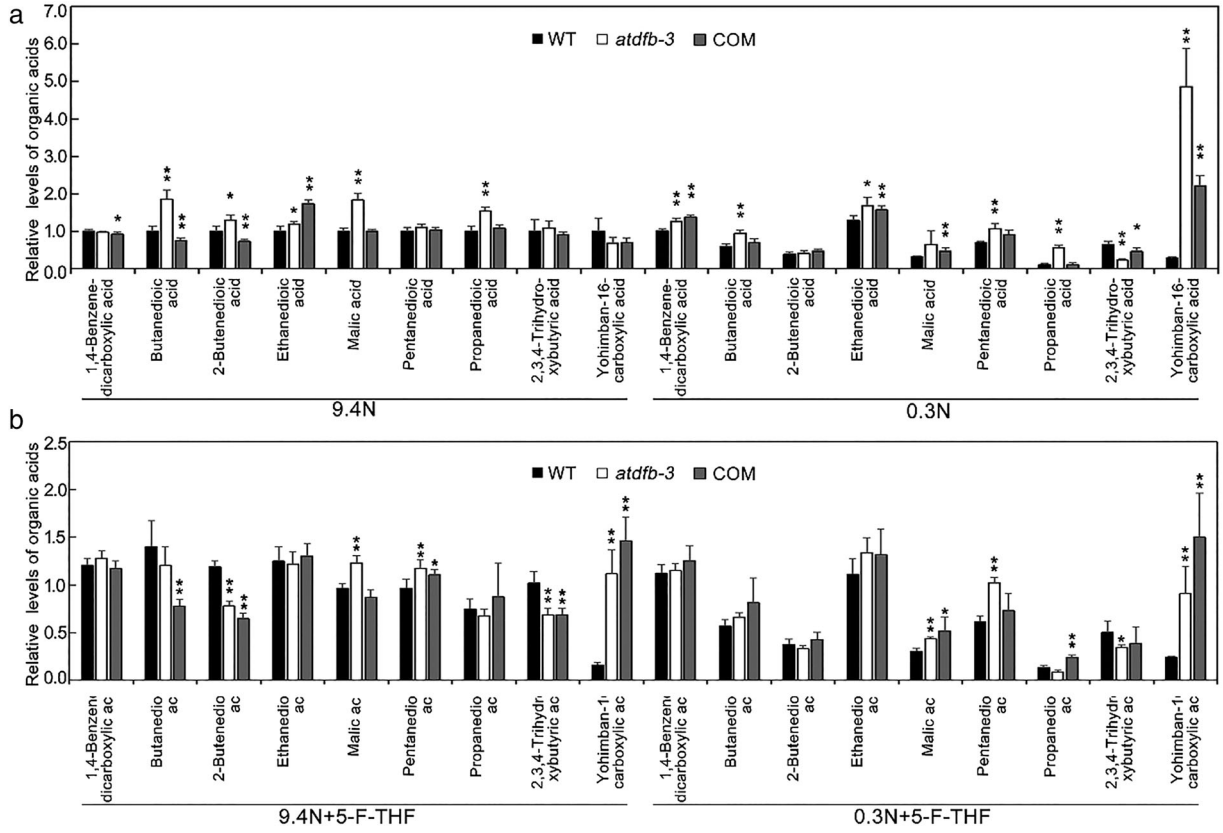

FIGURE 4 Relative levels of organic acids in 6-day-old etiolated wild-type, *atdfb-3*, and *AtDFB* complemented (COM) seedlings on 9.4- or .3-N medium (a), and 9.4- or .3-N medium with 5-F-THF (b). $n = 5$, and each replicate consisted of 100-mg pooled plant material. White bars with * indicate significant differences at $P < .05$, and those with ** indicate highly significant differences at $P < .01$ (Student's *t*-test).

THF to the medium decreased the differences between the *atdfb-3* and wild-type seedlings. The ratio of the butanedioic acid content between the *atdfb-3* and wild-type seedlings was 1.85 under the 9.4-N condition but was .86 under the 9.4 N + 5-F-THF condition. The addition of 5-F-THF to the .3-N medium caused the propanedioic acid and yohimban-16-carboxylic acid contents in the *atdfb-3* seedlings to respectively decrease to 15% and 19% of the corresponding levels in the *atdfb-3* seedlings grown on the .3 N medium. Thus, the ratios of the propanedioic acid and yohimban-16-carboxylic acid contents between the *atdfb-3* and wild-type seedlings were respectively 5.00 and 17.36 under the .3-N condition but were restored to .62 and 3.79 under the .3 N + 5-F-THF condition (Figure 4 and Tables S5 & S12).

3.2 | Nitrogen metabolites are affected by the *AtDFB* mutation

The *AtDFB* mutation resulted in a decrease in the carbon-to-nitrogen ratio (Figure S3), suggestive of a change in amino acid metabolism (Munoz-Bertomeu et al., 2009). Therefore, we examined the contents of individual amino acids *atdfb-3* seedlings grown under both nitrogen conditions with and without 5-F-THF supplementation. The total free amino acid contents were .82-fold and 1.05-fold higher in the *atdfb-3* mutant than in the wild-type control under the 9.4- and .3-N conditions, respectively (Figure 5a and Table S7). The addition of 5-F-THF to the 9.4-N medium caused the total free amino acid content in the *atdfb-3* seedlings to decrease to only 49% of that in the *atdfb-3* seedlings grown on the 9.4-N medium. Moreover, the ratio of the total free amino acid content between the *atdfb-3* and wild-type seedlings was 1.82 under the 9.4-N condition but was .90 under the 9.4 N + 5-F-THF condition. After 5-F-THF was added to the .3-N medium, the total free amino acid content decreased substantially in the *atdfb-3* and wild-type seedlings. The ratio of the total free amino acid content between the *atdfb-3* and wild-type seedlings was 2.05 under the .3-N condition but was 1.62 under the .3 N + 5-F-THF condition (Tables S7 and S14).

When nitrogen was sufficiently available, many amino acids, including Ser, Gln, Gly, Asp, Leu, Val, Pro, Thr, Ile, Lys, Asn, Arg, Orn, His, Phe, and a-Aba, accumulated to higher levels in the *atdfb-3* mutant than in the wild-type control (Figre 5b,c and Table S7). Specifically, the Ser and Asn contents were respectively 9.12-fold and 11.04-fold higher in the *atdfb-3* seedlings than in the wild-type seedlings. In contrast, Glu and Met were 55% less abundant in the mutant than in the wild-type control. The amounts of most free amino acids were similarly lower in the mutant and wild-type seedlings under the nitrate-limited condition than under the nitrate-sufficient condition (Table S7). As a result, many individual amino acids remained more

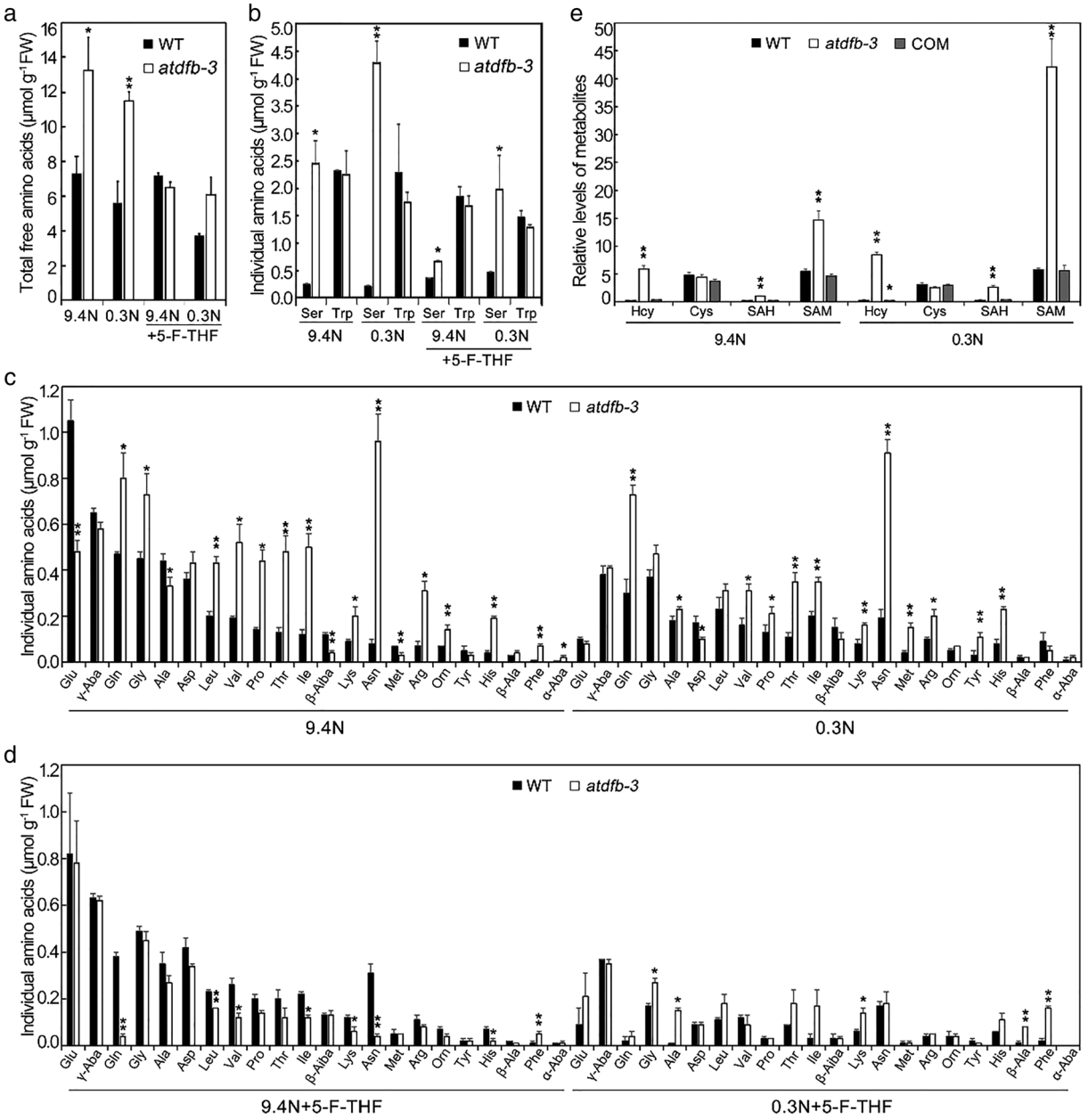

FIGURE 5 Amino acids and one-carbon metabolites in 6-day-old etiolated wild-type, *atdfb-3*, and *AtDFB* complemented (COM) seedlings on 9.4- or .3-N medium, and 9.4- or .3-N medium with 5-F-THF. (a) Total free amino acids contents. (b) Ser and Trp contents. (c, d) Individual amino acids content. (E) Relative levels of metabolites related to one-carbon metabolism. (a–d) $n = 3$, and each replicate consisted of 300-mg pooled plant material; (e) $n = 6$, and each replicate consisted of 50-mg pooled plant material. White bars with * indicate significant differences at $P < .05$, and those with ** indicate highly significant differences at $P < .01$ (Student's *t*-test).

abundant in the *atdfb-3* seedlings than in the wild-type seedlings. The exceptions included the Asp content in the mutant, which was only 59% of the amount in the wild-type control. The amounts of Met and Tyr increased in the *atdfb-3* seedlings to levels 2.75-fold and 2.67-fold higher than the corresponding levels in the wild-type seedlings. Additionally, the Ser content increased significantly in the *atdfb-3* mutant, and became the predominant free amino acid (Figure 5b,c and Table S7). These results indicate that the mutation to *AtDFB* enhanced the synthesis of amino acids during skotomorphogenesis in seedlings grown under both nitrogen conditions. The wild-type and *atdfb-3* seedlings responded differently to the addition of 5-F-THF to the 9.4-N medium (Figure 5c,d and Table S7). The contents of 16 amino acids decreased in the *atdfb-3* seedlings, but increased in the wild-type seedlings, whereas three amino acids (Glu, γ-Aba, and Met) accumulated in the *atdfb-3* mutant, but decreased in abundance in the wild-type control. An analysis of the Asn content revealed it decreased in the *atdfb-3* seedlings grown on the 9.4 N + 5-F-THF medium to only 4% of that of the *atdfb-3* seedlings grown on the 9.4-N medium. However, the Asn content was 2.88-fold higher in the wild-type seedlings grown on the 9.4 N + 5-F-THF medium than in

the wild-type seedlings grown on the 9.4-N medium. The variations in the Ser contents in the *atdfb-3* and wild-type seedlings were similar to the changes in the Asn levels. The ratios of the Asn and Ser contents between the *atdfb-3* and wild-type seedlings were respectively 12.00 and 10.17 under the 9.4-N condition, but were restored to .13 and 1.83 under the 9.4 N + 5-F-THF condition (Table S7). The inclusion of 5-F-THF in the .3-N medium greatly decreased the difference in the Asn and Ser contents between the *atdfb-3* and wild-type seedlings. The ratios of the Asn and Ser contents between the *atdfb-3* and wild-type seedlings were respectively 4.79 and 21.45 under the .3-N condition but were 1.06 and 4.30 under the .3 N + 5-F-THF condition. The differences in the abundance of five amino acids (i.e., Asp, Pro, β-Aiba, Met, and Orn) between the *atdfb-3* mutant and the wild-type control were eliminated in response to the addition of 5-F-THF (Figure 5c,d and Table S7). These results provide direct proof that folate contributes to seedling amino acid metabolism during skotomorphogenesis.

One-carbon metabolites, such as Hcy, SAM, and SAH, were highly accumulated in the mutant under both nitrogen conditions, whereas their contents in the COM line were restored to wild-type levels (Figure 5e and Table S8). This suggests that altered folate metabolism leads to the abnormal metabolism of one-carbon compounds that accumulate in the mutant.

4 | DISCUSSION

Folates, as one-carbon unit donors and acceptors, are involved in many enzymatic reactions, including the synthesis of methionine, purine, thymidine, pantothenate, and formyl-methionyl-tRNA, the transformation of glycine and serine, the catabolism of histidine, and the activation of formate (Hanson & Roje, 2001; Ravanel et al., 2004). Additionally, 5-methyl tetrahydrofolate (5-M-THF) is involved in the synthesis of the methyl donor SAM (Ravanel et al., 2004). The inhibition of folate synthesis by sulfadiazine leads to decreased genomic DNA methylation and folate contents in Arabidopsis (Zhang et al., 2012). A mutation in 5-formyltetrahydrofolate cycloligase (5-FCL, which participates in the conversion of folate derivatives to other compounds) decreases the growth rate of Arabidopsis plants by 20% and delays flowering by 1 week, but it increases the 5-F-THF, total folate, and Gly contents (Goyer et al., 2005). The deletion of the mitochondrial gene *AtDFC* (*FPGS2*) results in abnormal nitrogen metabolism in Arabidopsis seedlings as well as increased sensitivity to low-nitrogen stress. Compared with the wild-type control, the Gly and starch contents of the mutant reportedly increase under the low-nitrogen condition (Jiang et al., 2013). Earlier research confirmed that propanedioic acid is involved in fatty acid synthesis (Chen et al., 2011; Mu et al., 2008; Wu & Xue, 2010). Additionally, malic acid and 2-butenedioic acid participate in the tricarboxylic acid cycle, whereas campesterol is the precursor for brassinolide biosynthesis (He et al., 2003; Noguchi et al., 2000). These three processes share the same precursor (i.e., acyl-CoA). The accumulation of propanedioic acid, malic acid, and campesterol in the *atdfb-3* seedlings observed in this study likely reflects changes in fatty acid synthesis, tricarboxylic acid cycle, and brassinolide biosynthesis. Glucopyranoside, butanal, and 1,2-ethandimine are involved in secondary metabolism during plant development (Kai et al., 2006; Musthafa et al., 2013).

In this study, the altered folate metabolism in the *atdfb-3* mutant affected many metabolites, such as sugars, polyols, fatty acids, and amino acids, indicating that folate directly or indirectly participates in many pathways related to these metabolites. Folate may be in the form of a coenzyme or it may provide a carbon unit to certain reactions (e.g., Met synthesis).

Under the nitrogen-sufficient condition, the total folate, 5-M-THF, and 5-F-THF contents were lower in the *atdfb-3* seedlings than in the wild-type (Meng et al., 2014). Similarly, sugars (e.g., mannose), polyols (e.g., stigmasterol), and fatty acids (e.g., 9:0, 12:0, and 13:0) were less abundant in the *atdfb-3* mutant than in the wild-type control (Figures 1–3). The disrupted folate metabolism in the *atdfb-3* seedlings interfered with the synthesis or metabolism of sugars, polyols, and fatty acids. Under the nitrate-limited condition, the total folate and 5-M-THF contents were lower in the mutant than in the wild-type control, which is in contrast to the 5-F-THF content (Meng et al., 2014; Meng et al., 2017). Moreover, the mutant accumulated various metabolites, including fructose, galactose, glucopyranoside, mannose, campesterol, stigmasterol, and fatty acids (e.g., 18:3, 20:1, and 24:0). The elevated abundance of these metabolites may be related to the accumulation of 5-F-THF in the *atdfb-3* seedlings. It is also possible that insufficient nitrogen sources and altered folate metabolism affect these metabolic pathways and lead to the accumulation of specific metabolites.

Unlike the effects of the loss-of-function mutation to *AtDFB* on sugars, polyols, organic acids, and fatty acids, the total amino acid and various free amino acid contents were higher in the *atdfb-3* seedlings than in the wild-type seedlings; however, they were lower in the *atdfb-3* mutant than in the wild-type control when seedlings were grown on .9- and .3-N medium supplemented with 5-F-THF. Large amounts of amino groups may be converted to other compounds in the presence of folate to mediate skotomorphogenesis. The accumulation of SAH probably inhibits methyltransferase activity. The accumulation of the methyl donor SAM in the mutant in darkness is consistent with the results of an earlier study regarding the materials in plants cultivated under light (Zhou et al., 2013). The accumulation of SAM and SAH in the *atdfb-3* mutant was indicative of a decrease in the efficiency of the use of SAM by DNA methyltransferase, or SAM synthesis was perhaps more active in the *atdfb-3* mutant than in the wild type. The above-mentioned results imply that folate regulates multiple metabolic pathways related to carbon metabolism, nitrogen metabolism, and one-carbon metabolism during skotomorphogenesis, which provides novel insights into folate functions. The specific regulatory mechanism will need to be investigated in future studies.

The *atdfb-3* hypocotyl and root were significantly shorter than the wild-type and COM hypocotyls and roots, especially under the low-nitrogen condition (Meng et al., 2014; Meng et al., 2017). The short-root phenotype may make the mutant less able to absorb the nutrients in the medium than the wild-type control, further affecting

plant growth and metabolism. Furthermore, the disordered folate metabolism caused by the loss-of-function mutation to *AtDFB* in the *atdfb-3* mutant may directly or indirectly disturb other metabolic pathways, thereby exacerbating the short-hypocotyl and short-root phenotypes. Additionally, the accumulated seed reserves (e.g., galactose, mannose, and campesterol contents) in the *atdfb-3* mutant differed from those of the wild-type and COM samples, which may have affected the metabolite contents to some extent.

Previous studies indicated that *AtDFB* is normally expressed in COM plants (Meng et al., 2014) and the physiological characteristics (e.g., hypocotyl length) of COM plants are similar to those of the wild-type plants. However, we observed that the carbon metabolites of the COM seedlings were not restored to wild-type levels. There are several possible explanations for these results. First, the total folate contents in the COM seedlings were only 71% and 88% of the wild-type levels under the 9.4- and .3-N conditions, respectively (Meng et al., 2014). Second, under the N-sufficient condition, the 5-F-THF and 5-M-THF contents in the COM plants were respectively only 60% and 79% of the corresponding levels in the wild-type control. Third, the folate derivative profiles of the wild-type and COM plants respond differentially to the limited availability of N. For example, in a previous study, N limitation led to a 50% decrease in the 5-F-THF content of the wild-type seedlings, but had no effect on the 5-F-THF content in the COM seedlings, resulting in a 1.2-fold abundance of 5-F-THF in COM seedlings than in the wild-type control (Meng et al., 2014).

Due to the AtDFB catalyzes the extension of the Glu tail of the folate molecule (Ravanel et al., 2001), a mutated AtDFB alters the glutamylation status of some folate classes (Srivastava et al., 2011). 5-M-THF, one of folate derivatives, can only partially rescue abnormal hypocotyl elongation under N-limited conditions (Meng et al., 2014). Earlier investigations confirmed that 5-F-THF, which is an enzyme regulator (Roje et al., 2002) that mainly interacts with proteins associated with metabolic pathways, C1 metabolism, nitrogen fixation, sucrose biosynthesis, and translation (Li et al., 2021), can rescue the defective primary root development of the *atdfb* mutant under light (Jabrin et al., 2003; Srivastava et al., 2011) and dark (Meng et al., 2014) conditions. Additionally, 5-F-THF mediates the feedback regulation of folate biosynthesis (Li et al., 2021). Moreover, the dihydrofolate content reportedly increases by 1.00-fold in COM plants but decreases by 29% in wild-type plants, under the N-limited condition (Meng et al., 2014). Furthermore, AtDFB is the predominant isoform of FPGS downstream of dihydrofolate synthetase (Ravanel et al., 2001; Srivastava et al., 2011). We speculate that folate metabolism, which influences carbon metabolism, was not completely restored in the COM seedlings examined in this study.

5 | CONCLUSIONS

Our results indicate that altered folate metabolism affects the accumulation of sugars, polyols, organic acids, fatty acids, and amino acids in *atdfb-3* seedlings during skotomorphogenesis. A treatment with exogenous 5-F-THF decreases the differences in the contents of multiple metabolites between the *atdfb-3* mutant and the wild-type control. Overall, the data presented herein suggest that folate probably regulates or contributes to carbon and nitrogen metabolism.

ACKNOWLEDGMENTS

We thank Xiaoquan Qi and Lixin Duan in the Institute of Botany, Chinese Academy of Sciences for help with the metabolites analysis. We thank Jin Si in the Animal Nutrition and Feed Research Institute, Chinese Academy of Agricultural Sciences (CAAS) for help with the free amino acid analysis.

CONFLICT OF INTEREST

The authors declare that they have no conflict of interest.

AUTHOR CONTRIBUTIONS

X. L. and H. M. conceived the original research experiments and drafted the manuscript. L. L. and C. H. performed the experiments and analyzed the data. C. Z. wrote and edit the manuscript. All authors have read and agreed to the published version of the manuscript.

DATA AVAILABILITY STATEMENT

The datasets analyzed in this study are available from the corresponding author upon reasonable request.

ORCID

Xingjuan Li https://orcid.org/0000-0002-6338-9864

REFERENCES

Canas, R. A., de la Torre, F., Canovas, F. M., & Canton, F. R. (2006). High levels of asparagine synthetase in hypocotyls of pine seedlings suggest a role of the enzyme in re-allocation of seed-stored nitrogen. *Planta*, *224*, 83–95. https://doi.org/10.1007/s00425-005-0196-6

Chen, H., Kim, H. U., Weng, H., & Browse, J. (2011). Malonyl-CoA synthetase, encoded by ACYL ACTIVATING ENZYME13, is essential for growth and development of Arabidopsis. *Plant Cell*, *23*, 2247–2262. https://doi.org/10.1105/tpc.111.086140

Chen, M., & Thelen, J. J. (2010). The plastid isoform of triose phosphate isomerase is required for the postgerminative transition from heterotrophic to autotrophic growth in Arabidopsis. *Plant Cell*, *22*, 77–90. https://doi.org/10.1105/tpc.109.071837

Collakova, E., Goyer, A., Naponelli, V., Krassovskaya, I., Gregory, J. F. 3rd, Hanson, A. D., & Shachar-Hill, Y. (2008). Arabidopsis 10-formyl tetrahydrofolate deformylases are essential for photorespiratio. *Plant Cell*, *20*, 1818–1832. https://doi.org/10.1105/tpc.108.058701

Eastmond, P. J., Germain, V., Lange, P. R., Bryce, J. H., Smith, S. M., & Graham, I. A. (2000). Postgerminative growth and lipid catabolism in oilseeds lacking the glyoxylate cycle. *Proceedings of the National Academy of Sciences of the United States of America*, *97*, 5669–5674. https://doi.org/10.1073/pnas.97.10.5669

Goyer, A., Collakova, E., Diaz de la Garza, R., Quinlivan, E. P., Williamson, J., Gregory, J. F., Shachar-Hill, Y., & Hanson, A. D. (2005). 5-Formyltetrahydrofolate is an inhibitory but well tolerated metabolite in Arabidopsis leaves. *The Journal of Biological Chemistry*, *280*, 26137–26142. https://doi.org/10.1074/jbc.M503106200

Hanson, A. D., & Gregory, J. F. (2002). Synthesis and turnover of folates in plants. *Current Opinion in Plant Biology*, *5*, 244–249. https://doi.org/10.1016/S1369-5266(02)00249-2

Hanson, A. D., & Gregory, J. F. (2011). Folate biosynthesis, turnover, and transport in plants. *Annual Review of Plant Biology*, *62*, 105–125. https://doi.org/10.1146/annurev-arplant-042110-103819

Hanson, A. D., & Roje, S. (2001). One-carbon metabolism in higher plants. *Annual Review of Plant Physiology and Plant Molecular Biology*, *52*, 119–137. https://doi.org/10.1146/annurev.arplant.52.1.119

Hayashi, M., Tanaka, M., Yamamoto, S., Nakagawa, T., Kanai, M., Anegawa, A., Ohnishi, M., Mimura, T., & Nishimura, M. (2017). Plastidial folate prevents starch biosynthesis triggered by sugar influx into non-photosynthetic plastids of Arabidopsis. *Plant and Cell Physiology*, *58*, 1328–1338. https://doi.org/10.1093/pcp/pcx076

He, J. X., Fujioka, S., Li, T. C., Kang, S. G., Seto, H., Takatsuto, S., Yoshida, S., & Jang, J. C. (2003). Sterols regulate development and gene expression in Arabidopsis. *Plant Physiology*, *131*, 1258–1269. https://doi.org/10.1104/pp.014605

Jabrin, S., Ravanel, S., Gambonnet, B., Douce, R., & Re'beille, F. (2003). One-carbon metabolism in plants. Regulation of tetrahydrofolate synthesis during germina-tion and seedling development. *Plant Physiology*, *131*, 1431–1439.

Jiang, L., Liu, Y., Sun, H., Han, Y., Li, J., Li, C., Guo, W., Meng, H., Li, S., Fan, Y., & Zhang, C. (2013). The mitochondrial folylpolyglutamate synthetase gene is required for nitrogen utilization during early seedling development in arabidopsis. *Physiology*, *161*, 971–989.

Jin, H., Li, H., & Zhu, Z. (2021). Experimental procedures for studying skotomorphogenesis in arabidopsis thaliana. *Methods in Molecular Biology*, *6*, 49–60.

Josse, E. M., & Halliday, K. J. (2008). Skotomorphogenesis: The dark side of light signalling. *Current Biology*, *18*, 1144–1146.

Kai, K., Shimizu, B., Mizutani, M., Watanabe, K., & Sakata, K. (2006). Accumulation of coumarins in Arabidopsis thaliana. *Phytochemistry*, *67*, 379–386. https://doi.org/10.1016/j.phytochem.2005.11.006

Kushwah, S., & Laxmi, A. (2014). The interaction between glucose and cytokinin signal transduction pathway in Arabidopsis thaliana. *Plant, Cell and Environment*, *37*, 235–253. https://doi.org/10.1111/pce.12149

Li, C., Zheng, L. L., Wang, X. N., Hu, Z. B., Zheng, Y., Chen, Q. H., Hao, X. C., Xiao, X., Wang, X. B., Wang, G. D., & Zhang, Y. H. (2019). Comprehensive expression analysis of arabidopsis GA2-oxidase genes and their functional insights. *Plant Science*, *285*, 1–13. https://doi.org/10.1016/j.plantsci.2019.04.023

Li, W. C., Liang, Q. J., Chandra, M. R., Raul, S. M., Wang, H., Chen, X., Dominique, V. D., Zhang, C. Y., & Xiao, Y. L. (2021). The 5-formyltetrahydrofolate proteome links folates with c/n metabolism and reveals feedback regulation of folate biosynthesis. *The Plant Cell*, *33*, 3367–3385. https://doi.org/10.1093/plcell/koab198

Liu, W., Han, T., Yuan, H., Yu, Z., & Lu, Y. (2017). Catalase2 functions for seedling post-germinative growth by scavenging H_2O_2 and stimulating ACX2/3 activity in arabidopsis: Catalase2 functions in early seedling growth. *Plant, Cell and Environment*, *40*, 2720–2728. https://doi.org/10.1111/pce.13031

Meng, H., Jiang, L., Xu, B., Guo, W., Li, J., Zhu, X., Qi, X., Duan, L., Meng, X., Fan, Y., & Zhang, C. (2014). Arabidopsis plastidial folylpolyglutamate synthetase is required for seed reserve accumulation and seedling establishment in darkness. *PLoS ONE*, *9*, e101905. https://doi.org/10.1371/journal.pone.0101905

Meng, H., Xu, B., Zhang, C., & Jiang, L. (2017). Arabidopsis plastidial folylpolyglutamate synthetase is required for nitrogen metabolism under nitrate-limited condition in darkness. *Biochemical and Biophysical Research Communications*, *482*, 277–281. https://doi.org/10.1016/j.bbrc.2016.11.054

Mu, J., Tan, H., Zheng, Q., Fu, F., Liang, Y., Zhang, J., Yang, X., Wang, T., Chong, K., Wang, X. J., & Zuo, J. (2008). LEAFY COTYLEDON1 is a key regulator of fatty acid biosynthesis in Arabidopsis. *Plant Physiology*, *148*, 1042–1054. https://doi.org/10.1104/pp.108.126342

Munoz-Bertomeu, J., Cascales-Minana, B., Mulet, J. M., Baroja-Fernandez, E., Pozueta-Romero, J., Kuhn, J. M., Segura, J., & Ros, R. (2009). Plastidial glyceraldehyde-3-phosphate dehydrogenase deficiency leads to altered root development and affects the sugar and amino acid balance in Arabidopsis. *Plant Physiology*, *151*, 541–558. https://doi.org/10.1104/pp.109.143701

Musthafa, K. S., Sahu, S. K., Ravi, A. V., & Kathiresan, K. (2013). Anti-quorum sensing potential of the mangrove Rhizophora annamalayana. *World Journal of Microbiology and Biotechnology*, *29*, 1851–1858.

Nikiforova, V. J., Kopka, J., Tolstikov, V., Fiehn, O., Hopkins, L., Hawkesford, M. J., Hesse, H., & Hoefgen, R. (2005). Systems rebalancing of metabolism in response to sulfur deprivation, as revealed by metabolome analysis of Arabidopsis plants. *Plant Physiology*, *138*, 304–318. https://doi.org/10.1104/pp.104.053793

Noguchi, T., Fujioka, S., Choe, S., Takatsuto, S., Tax, F. E., Yoshida, S., & Feldmann, K. A. (2000). Biosynthetic pathways of brassinolide in Arabidopsis. *Plant Physiology*, *124*, 201–209. https://doi.org/10.1104/pp.124.1.201

O'Neill, C. M., Gill, S., Hobbs, D., Morgan, C., & Bancroft, I. (2003). Natural variation for seed oil composition in Arabidopsis thaliana. *Phytochemistry*, *64*, 1077–1090. https://doi.org/10.1016/S0031-9422(03)00351-0

Penfield, S., Rylott, E. L., Gilday, A. D., Graham, S., Larson, T. R., & Graham, I. A. (2004). Reserve mobilization in the Arabidopsis endosperm fuels hypocotyl elongation in the dark, is independent of abscisic acid, and requires PHOSPHOENOLPYRUVATE CARBOXYKINASE1. *Plant Cell*, *16*, 2705–2718. https://doi.org/10.1105/tpc.104.024711

Ravanel, S., Block, M. A., Rippert, P., Jabrin, S., Curien, G., Rebeille, F., & Douce, R. (2004). Methionine metabolism in plants: Chloroplasts are autonomous for de novo methionine synthesis and can import S-adenosylmethionine from the cytosol. *The Journal of Biological Chemistry*, *279*, 22548–22557. https://doi.org/10.1074/jbc.M313250200

Ravanel, S., Cherest, H., Jabrin, S., Grunwald, D., Surdin-Kerjan, Y., Douce, R., & Rebeille, F. (2001). Tetrahydrofolate biosynthesis in plants: Molecular and functional characterization of dihydrofolate synthetase and three isoforms of folylpolyglutamate synthetase in Arabidopsis thaliana. *Proceedings of the Academy of Sciences of the United States of America*, *98*, 15360–15365.

Renault, H., El Amrani, A., Palanivelu, R., Updegraff, E. P., Yu, A., Renou, J. P., Preuss, D., Bouchereau, A., & Deleu, C. (2011). GABA accumulation causes cell elongation defects and a decrease in expression of genes encoding secreted and cell wall-related proteins in Arabidopsis thaliana. *Plant and Cell Physiology*, *52*, 894–908. https://doi.org/10.1093/pcp/pcr041

Roje, S., Janave, M. T., Ziemak, M. J., & Hanson, A. D. (2002). Cloning and characterization of mitochondrial 5-formyltetrahydrofolate cycloligase from higher plants. *Journal of Biological Chemistry*, *277*, 42748–42754. https://doi.org/10.1074/jbc.M205632200

Sahr, T., Ravanel, S., & Rebeille, F. (2005). Tetrahydrofolate biosynthesis and distribution in higher plants. *Biochemical Society Transactions*, *33*, 758–762. https://doi.org/10.1042/BST0330758

Sallam, S. M., Shawky, E., & Sohafy, S. (2021). Determination of the effect of germination on the folate content of the seeds of some legumes using HPTLC-mass spectrometry-multivariate image analysis. *Food Chemistry*, *362*, 130206. https://doi.org/10.1016/j.foodchem.2021.130206

Srivastava, A. C., Ramos-Parra, P. A., Bedair, M., Robledo-Hernandez, A. L., Tang, Y., Sumner, L. W., Diaz de la Garza, R. I., & Blancaflor, E. B. (2011). The folylpolyglutamate synthetase plastidial isoform is required for postembryonic root development in Arabidopsis. *Plant Physiology*, *155*, 1237–1251. https://doi.org/10.1104/pp.110.168278

Van Wilder, V., De Brouwer, V., Loizeau, K., Gambonnet, B., Albrieux, C., Van Der Straeten, D., Lambert, W. E., Douce, R., Block, M. A., Rebeille, F., & Ravanel, S. (2009). C1 metabolism and chlorophyll synthesis: The Mg-protoporphyrin IX methyltransferase activity is dependent on the folate status. *New Phytologist*, *182*, 137–145. https://doi.org/10.1111/j.1469-8137.2008.02707.x

Wu, G. Z., & Xue, H. W. (2010). Arabidopsis beta-ketoacyl-[acyl carrier protein] synthase i is crucial for fatty acid synthesis and plays a role in chloroplast division and embryo development. *Plant Cell*, *22*, 3726–3744. https://doi.org/10.1105/tpc.110.075564

Xu, Z., Wang, M., Shi, D., Zhou, G., Niu, T., Hahn, M. G., O'Neill, M. A., & Kong, Y. (2017). DGE-seq analysis of MUR3 -related arabidopsis mutants provides insight into how dysfunctional xyloglucan affects cell elongation. *Plant Science*, *258*, 156–169.

Zhang, H., Deng, X., Miki, D., Cutler, S., La, H., Hou, Y. J., Oh, J., & Zhu, J. K. (2012). Sulfamethazine suppresses epigenetic silencing in Arabidopsis by impairing folate synthesis. *Plant Cell*, *24*, 1230–1241. https://doi.org/10.1105/tpc.112.096149

Zhang, Y., Liu, Z., Wang, L., Zheng, S., Xie, J., & Bi, Y. (2010). Sucrose-induced hypocotyl elongation of Arabidopsis seedlings in darkness depends on the presence of gibberellins. *Journal of Plant Physiology*, *167*, 1130–1136. https://doi.org/10.1016/j.jplph.2010.03.007

Zhong, C., Jian, S. F., Chen, D. L., Huang, X. J., & Miao, J. H. (2021). Organic nitrogen sources promote andrographolide biosynthesis by reducing nitrogen metabolism and increasing carbon accumulation in andrographis paniculata. *Plant Physiology and Biochemistry*, *164*, 82–91. https://doi.org/10.1016/j.plaphy.2021.04.016

Zhou, H. R., Zhang, F. F., Ma, Z. Y., Huang, H. W., Jiang, L., Cai, T., Zhu, J. K., Zhang, C., & He, X. J. (2013). Folate polyglutamylation is involved in chromatin silencing by maintaining global DNA methylation and histone H3K9 dimethylation in Arabidopsis. *Plant Cell*, *25*, 2545–2559. https://doi.org/10.1105/tpc.113.114678

SUPPORTING INFORMATION

Additional supporting information can be found online in the Supporting Information section at the end of this article.

How to cite this article: Li, X., Meng, H., Liu, L., Hong, C., & Zhang, C. (2022). Metabolic network changes during skotomorphogenesis in *Arabidopsis thaliana* mutant (*atdfb-3*). *Plant Direct*, *6*(11), e00467. https://doi.org/10.1002/pld3.467